Simultaneous Measurement of Ionic and Electronic Conductivities of Conductive Polymers as a Function of Electrochemical Doping in Battery Electrolyte

*Billal Zayat, Pratyusha Das, Barry C. Thompson, and Sri R. Narayan**

Department of Chemistry and Loker Hydrocarbon Research Institute, University of Southern California, Los Angeles, California 90089-1661, USA

ABSTRACT

Conductive polymers are increasingly being studied as additives in lithium-ion batteries, supercapacitors and other electrochemical devices due to their ability to conduct electrons and ions, and serve as binders. These polymers undergo electrochemical doping during battery cycling along with swelling by the electrolyte solvent, whereupon the ionic and electronic conductivities change by several orders of magnitude. Measuring these large changes as a function of electrochemical doping, in a relevant electrolyte, has been a challenge thus far. We show that the ionic and electronic conductivity of a wide range of p-type and n-type conducting polymer thin films can be reliably measured as a function of electrochemical doping in relevant battery electrolytes by impedance spectroscopy on interdigitated electrodes by combining two separate electrode geometries. The results demonstrate the broad applicability of the methodology for gaining insights into the electrical conduction in polymers in relevant environments, particularly for batteries and other electrochemical devices.

INTRODUCTION

Conductive Polymers as Multifunctional Binders. Lithium-ion batteries have become the dominant energy storage technology for portable devices and electric vehicles due to the relatively high specific energy and power density of these batteries [1-3]. The electrodes in these batteries employ traditionally, mechanical binders such as polyvinylidene fluoride (PVDF) that are electrical insulators. Due to their insulating nature, such binders tend to hinder charge transport in the electrodes leading to a reduced performance.[4-6] Consequently, conductive polymers have been extensively explored as binders for both low and high-voltage electrodes in LIBs due to their superior ion and electron transport properties.[7-24] Due to their significant impact on performance, conducting polymers have also been investigated in lithium-sulfur batteries, supercapacitors, and pseudocapacitors.[25-29] Furthermore, nanostructured conducting polymers have garnered much attention as active materials in organic electrodes.[30] Thin films of neutral conjugated polymers such as poly(3-hexylthiophene) (P3HT) and poly{[*N*,*N*′-bis(2-octyldodecyl)-naphthalene-1,4,5,8-bis(dicarboximide)-2,6-diyl]-*alt*-5,5′-(2,2′-bithiophene)} (P(NDI2OD-T2)) are rendered electronically conductive when either electro-oxidation or electro-reduction generates mobile charge carriers, typically described as polarons and bipolarons. Simultaneously, counter ions are introduced into the polymer structure for ensuring charge compensation.[31, 32] This process by which the polymer becomes electrically conducting is often referred to as "electrochemical doping". Electro-oxidation and electro-reduction produce "p-doped" polymers or "n-doped" polymers, respectively. The doping process results in remarkable changes in electronic conductivity spanning several orders of magnitude. For example, electrochemical doping increases the electronic conductivity of poly(3-hexylthiophene)-poly(ethylene oxide) (P3HT-PEO) block copolymer from 10^{-8} to 10^{-2} S cm^{-1}.[33] Similarly, the structural and morphological changes induced

by electrochemical doping can be expected to alter the ionic conductivity in these polymers. When the conductive polymer is part of a battery electrode, the changes in electrical conductivity occur simultaneously with the charging and discharging of the electrode. The degree of doping and the number of charge carriers is controlled by holding the electrode potential at various values at which electro-oxidation or electro-reduction occur. We achieve optimal battery performance when the polymer remains in an electrically conductive state and is chemically stable over the entire operating potential window of the battery electrode. Although changes to the ionic conductivity are also expected, the effect of electrochemical doping is relatively unexplored. Such ionic conductivity changes are also very likely to influence the observed battery performance. Thus, measuring the electronic and ionic conductivity of the polymer thin films in the relevant battery electrolyte as a function of potential (i.e. electrochemical doping) will not only help explain the observed changes in battery electrode performance,[34] but will be a useful in gaining fundamental insights for the rational design of the next generation of conducting polymer binders and additives for various electrochemical devices.[33] The focus of the present study is on developing and demonstrating a reliable experimental method for such measurements.

Considerations for Measuring Electronic and Ionic Conductivity. There are several considerations for measuring the electrical conductivity of conductive polymers for battery applications: (1) The carbon additive usually present in battery electrodes masks the electronic conductivity contribution from the polymer binder necessitating a carbon-free electrode for studying just the polymer's properties, (2) We must be able to vary the electrode potential over the specific operating potential window of the battery electrode, (3) Measurements must be made in the relevant solvent and electrolyte so as to include the effect of swelling by the solvent, well known to alter the polymer's properties,[35, 36] and (4) Uniform electrochemical doping necessitates

a film that is a few tens of nanometers thick, so that the dopant anions or cations can access the entire volume of the film. Thus, a routine four-probe conductivity measurement on a film formed on an insulating planar substrate, an arrangement often used in electrical property measurements of thermoelectric materials, is inadequate for studying the electrochemical doping of conductive polymers.[37, 38]

Additional practical considerations are: (1) The electronic conductivity of polymers in the doped state can reach values greater than 1 S cm^{-1}, leading to a very small resistance across a thin film. Consequently, the voltage drop across these films will be too small to be reliably measured without using large currents. (2) The technique should have the dynamic measurement range to accommodate a change of several orders of magnitude in the electronic conductivity of the polymers when transitioning from an un-doped to a doped polymer. Thus, we need an electrode arrangement that combines the ability to perform *in situ* electrochemical doping on a thin polymer film and have a wide dynamic range of sensitivity.

In addition to electronic conductivity, values of ionic conductivity are also expected to change over a wide range with doping. The ionic conductivity values are usually three to four orders of magnitude lower than that of electronic conductivity, yet important in achieving the required battery performance. Thus, the measurement of both ionic and electronic conductivity using a single experimental setup presents a challenge. Specifically, we require the ability to switch between two separate geometries to enable measurement of very large and very small resistance values. A large thickness and small area of cross-section are needed for measuring low resistivity, while for measuring high resistivity, a thin layer with a large area of cross-section is desirable. Thus, meeting these conflicting requirements of electrode geometry is also a challenge.

Limitations of Currently Used Methods. In reviewing the literature we found several reports of the measurement of ionic and electronic conductivity of polymers.[39-43] However, none of these reported methods are suited for measuring and separating electronic and ionic conductivity of polymer thin films *simultaneously as a function of electrochemical doping in a relevant electrolyte*. For example, the electronic conductivity of a conductive block copolymer has been reported as a function of electrochemical doping by using electrochemical impedance spectroscopy (EIS) but the measurement was performed on a thick polymer film (over 100 μm) in a solid-state system, free of liquid electrolyte, and without the ability to measure ionic conductivity.[33] On the other hand, ionic and electronic conductivity of polymer thin films in LIB electrolyte has been reported simultaneously but without chemical or electrochemical doping.[44] EIS has also been successfully used to determine the ionic conductivity of polythiophene derivatives, but the salts were simply mixed with the polymer and then cast as a film, without any electrochemical doping.[45] In Table 1 we elaborate on the strengths and limitations of previously reported methods. Briefly, the previously-used techniques are limited in their ability to measure both electronic and ionic conductivity simultaneously, as a function of progressive electrochemical doping of the polymer, and in relevant electrolyte environments for battery applications.

Table 1. Comparison of Various Conductivity Measurement Methods

Technique	Brief Description/ Example	Advantages	Disadvantages
Four-Probe	4 electrodes attached to film on insulating substrate. Used for various applications such as OTFT's[46]	Geometry ideal for measuring electronic conductivity of thin films	Electrode geometry inappropriate for electrochemical doping. Not suited for measurement of ionic conductivity. Performed typically on dry film not in contact with liquid electrolyte.
EIS with blocking electrodes (Huggins Approach)	Yields dual ionic and electronic conductivity between two ion-blocking electrodes. P3HT-PEO block copolymer conductivity as a function of Li-salt mixing and ratio of PEO/P3HT[47]	Can simultaneously obtain ionic and electronic conductivity as a function of chemical doping	Electrode geometry inappropriate for electrochemical doping. Thick polymer film needed if conductivity is high. Both conductivities can only be obtained when similar in magnitude.
EIS + Electrochemical Doping	Huggins approach is used P3HT-PEO block copolymer electronic conductivity as a function of electrochemical doping using a 3 electrode cell[33]	Can obtain electronic conductivity as a function of electrochemical doping	Thick polymer films needed (>100 microns) Block copolymer with high ionic transport needed No liquid electrolyte Ionic conductivity only obtained when polymer is undoped Only electronic conductivity is obtained as a function of electrochemical doping
EIS + Interdigitated Microelectrode (IDM)	EIS to obtain ionic conductivity of polymer thin films on IDM[45]	IDM enhances signal A thin film can be used Conductivity can be obtained as a function of chemical doping	Geometry inappropriate for electrochemical doping When either conductivity dominates, the other conductivity value cannot be determined No liquid electrolyte can be used
Transmission Line Model	Suited for ionic conductivity measurements of thin films. Ionic conductivity of PEDOT:PSS mixed with PEO thin films was obtained[44]	Can obtain ionic conductivity of polymer thin films in liquid electrolyte	Electronic conductivity is not obtained Ionic conductivity was not reported as a function of electrochemical doping
This Work	Uses polymer thin film on IDM Allows for electrochemical doping in LIB electrolyte 2-probe measurement to determine electronic conductivity in LIB electrolyte at various potentials 3-electrode measurement to determine ionic conductivity at any given potential	Electronic conductivities up to 10 S cm^{-1} and ionic conductivities up to 10^{-3} S cm^{-1} can be measured (based on electrode geometry) The difference in orders of magnitude between ionic and electronic conductivities does not affect measurement Can be used with different LIB electrolytes	Upper limit of conductivity measurement is dictated by electrode dimensions. Polymer should be insoluble in liquid electrolyte

EXPERIMENTAL METHODS

Electrode Preparation. Interdigitated microelectrodes (IDM) were purchased from Metrohm Dropsens (DRP-G-IDEAU5-U20) and were rinsed with isopropanol and dried under argon before use. The electrode is composed of two interdigitated gold electrodes with two connection tracks on a glass substrate (L 22.8 × W 7.6 × H 0.7 mm). Each microelectrode is composed of 250 digits with a digit length of 6760 μm and a gap of 5 μm between the digits.

P3HT (85-100 kDa MW) and PEO (100 kDa average Mw) were purchased in powder form from Sigma-Aldrich. PEDOT:PSS (Clevios PH 1000) aqueous solution was purchased from Heraeus and used as received. P(NDI2OD-T2) was synthesized and purified as described in SI-2. Polymer solutions (20 mg mL^{-1}) of P3HT, PEO, and P(NDI2OD-T2) were prepared by dissolving the polymer in 1,2-dichlorobenzene (99%, Sigma-Aldrich). The solution was then heated at 40°C under argon for two hours to ensure complete dissolution of the polymer in the solvent. To prepare the P3HT/PEO sample, equal amounts of the solution of P3HT and PEO were mixed.

5 μL of the prepared solutions were spin-coated on the gold IDM at 1000 RPM for 30 seconds to produce a 50 nm polymer film (Figure 1a). The prepared electrodes were then annealed under vacuum at 110°C for two hours then transferred to a nitrogen glovebox. At least three IDMs were prepared for each polymer sample.

Electrochemical Doping. All electrochemical tests were performed in a nitrogen glovebox at room temperature. A 3-electrode cell (Figure 1b) was assembled in a nitrogen glovebox to electrochemically dope the polymer and determine its ionic conductivity. The two terminals of the interdigitated gold electrodes were shorted to form the working electrode. Pieces of lithium foil were used as the counter and reference electrodes. 1 M Bis(trifluoromethane)sulfonimide lithium salt (LiTFSI) in a mixture of 1:1 by volume of ethylene carbonate and dimethyl carbonate

(EC/DMC) was used as the electrolyte. To electrochemically dope the polymer, the potential of the working electrode was held for 300 seconds. This length of time ensured that the current decayed to an immeasurably low value ensuring that the doping process at that potential was complete. The potential was then stepped up to the next value. The range of the polarization varied with the polymer studied.

Cyclic Voltammetry. CV scans of the polymer films were performed to identify the generation of the polarons and bipolarons and determine the potential window of electrochemical doping. The IDM was held in the electrochemical doping configuration (Figure 1b), and the electrode potential was scanned repeatedly in a cyclic fashion at a preset scan rate in the range of 1 to 100 mV s^{-1} over a chosen window of electrode potential based on the polymer type. The current response was recorded as a function of the electrode potential, and the potentials corresponding to the current peaks were noted.

Electrochemical Impedance Measurements. To determine ionic conductivity, the impedance of the electrode was measured as a function of frequency (100 kHz to 100 mHz) at a sinusoidal excitation of ±10 mV peak-to-peak at each value of electrode potential of doping (Figure 2b). The potentiostatic EIS measurement was repeated at different values of electrode potential to determine the change in ionic conductivity as a function of degree of doping.

To measure the electronic conductivity accurately, the impedance measurement was carried out between the terminals of the two interdigitated gold electrodes. As shown in Figure 3a, electrochemical doping of the polymers was performed in the 3-electrode configuration as before and the cell was allowed to relax for 100 seconds to reach an equilibrium value. Following the doping process, the electrode connections were switched from the 3-electrode configuration to a

2-electrode configuration (Figure 3b). EIS measurement was then performed at open circuit potential between 100 mHz and 100 kHz at a sinusoidal excitation of ± 10 mV peak-to-peak.

RESULTS AND DISCUSSION

Electrode Geometry and Methodology to Measure Electronic and Ionic Conductivity. To allow for concurrently evaluating electronic and ionic conductivity as a function of electrochemical doping in liquid electrolyte, we have combined the merits of using the *planar* and *interdigitated* electrode geometry with EIS measurements. The test electrode is an interdigitated gold electrode with two terminals. The electrode is coated with a thin layer of the polymer film (Figure 1a). The two gold-electrode terminals are electrically shorted and the electrochemical doping is carried out by polarizing this test electrode in a three-electrode cell configuration in a solution of lithium-ion battery electrolyte at various potentials (Figure 1b, Figure 2). We also conducted cyclic voltammetry (CV) scans on the interdigitated electrode in the three-electrode configuration to track the electrochemical doping process and identify the electrode potentials at which the doping occurs (Figures 2a, S9a, S9b). Ionic conductivity of the film is measured in this three-electrode configuration using EIS (Figure 2c). The electrode geometry under these conditions is that of a planar electrode of large area and a small thickness, well suited for measuring large resistivity values (Figure S7b). After measuring the ionic conductivity, in a separate experiment on the same film, the electronic conductivity is measured between the terminals of the two gold interdigitated electrodes (Figure 3b). In this two-electrode geometry, the area of cross-section is small as governed by the thickness of the film, while the path length for current is long as determined by the distance between the digits of the gold electrodes (Figure S7a). The latter

geometry was well-suited for measuring very low values of resistivity. The EIS results were analyzed using appropriate electrical equivalent circuit models to yield the conductivity values (Figure 3).

Method Validation with Various Conducting Polymers. To validate the technique, we studied model systems of p-dopable and n-dopable polymers. We have used P3HT, 1:1 P3HT/PEO mixture, and poly(3,4-ethylenedioxythiophene)/poly(4-styrenesulfonate) (PEDOT:PSS) as the model p-dopable polymers, while P(NDI2OD-T2) was used as a model n-dopable polymer.

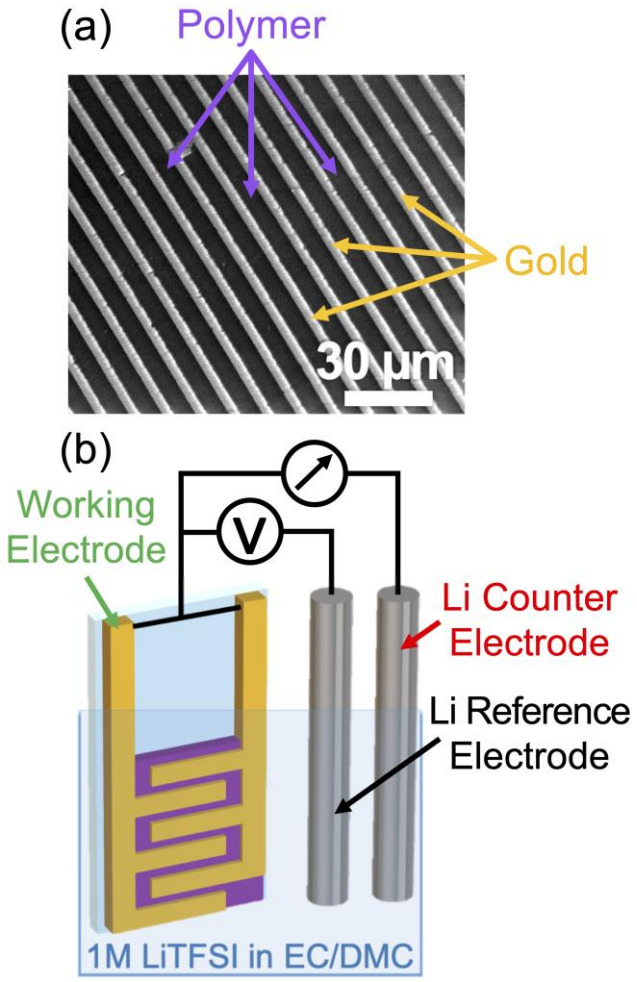

Figure 1. (a) SEM image of spin-coated P3HT on the gold interdigitated electrode. (b) The three-electrode configuration used to electrochemically dope the polymer and determine its ionic conductivity.

Cyclic voltammetry of P3HT films showed two current peaks at 3.45 V and 3.85 V vs. Li^+/Li, attributed to the formation of polaron and bipolarons, respectively (Figure 2a).[48] The CV scans of P3HT/PEO (Figure S9a) show similar oxidation peaks to those of P3HT while the CV scans of PEDOT:PSS (Figure S9b) showed no oxidation peaks in the examined potential window as expected as PEDOT:PSS was in the doped state by oxidation in air. In addition, the electrochemical doping of the P(NDI2OD-T2) film (Figure 4a) was observed in the potential range of 1.7 V to 3.0 V vs Li^+/Li.

Ionic Conductivity Measurements. The impedance of the polymer thin film electrodes was measured in the three-electrode configuration following electrochemical doping to different levels (Figure 2c). The sinusoidal potential perturbation is accompanied by double-layer charging, charge-transfer, diffusion and migration of ions, and the transport of electrons. The impedance response arising from these processes distributed across the thickness of the porous polymer film has been analyzed rigorously by Garcia-Belmonte *et al*.[49-51] Under these conditions the electrode impedance can be represented by a "finite length" transmission line model with a reflective boundary.[52, 53] This model with distributed circuit elements has been applied successfully to study the diffusion of charge carriers in electrochemically-doped thin polymer films.[54] For a 100 nm thick polymer film, the sinusoidal response at low frequencies (10 Hz to 0.1 Hz) arises from the entire volume and finite thickness of the porous film. Specifically, the ionic resistance of the polymer phase (R_{ion}), the electronic resistance of polymer phase (R_e), and the interfacial faradaic impedance (Z_f) are distributed circuit elements of a generalized transmission line equivalent circuit along with a geometric capacitance C_G of the entire thin film (Figure S8a). For such a model, assuming rapid interfacial charge-transfer, it was shown by Albery et al[52] that at low frequencies, the real component of the impedance Z_{real} tends to attain a constant value given by Eq. 1.

$$Z_{real} = \frac{R_{ion} + R_e}{3} + R_s \quad (1)$$

Here R_s is the uncompensated solution resistance obtained from the high frequency intercept. The value of Z_{real} was obtained by extrapolation of the low-frequency line to meet the real axis of the Nyquist plot (Figure S8b). With the electronic resistance R_e obtained separately (from the electronic conductivity measurement described in the next section), R_{ion} was obtained using Eq. 1.

The ionic conductivity of the polymer film, σ_{ion} was then calculated using Eq. 2, based on the dimensions of the electrode.

$$\sigma_{ion} = \frac{1}{R_{ion}} \times \frac{h}{l \times (N-1) \times d} \quad (2)$$

In Eq. 2, h is the thickness of the polymer film, l and N are the length and the number of the digits of the gold electrode, respectively, and d is the distance between the gold electrodes. To validate the measurement method and analysis, we studied various conjugated polymer films. For films of P3HT, at 3.0 V, prior to any significant doping, the ionic conductivity was 1×10^{-9} S cm^{-1} (Figure 2d). No ionic conductivity data of un-doped P3HT films could be found in the literature. This low value of ionic conductivity is not surprising as the un-doped P3HT film is semi-crystalline and lacks the ability to solvate Li^+ or anions. Upon electrochemical doping at a potential of 3.4 V vs Li^+/Li, anions were introduced into the polymer film, and the ionic conductivity of P3HT increased by an order of magnitude to 3×10^{-8} S cm^{-1}. The large decrease in impedance is evident in the Bode and Nyquist plots of the P3HT film (Figure S11). The ionic conductivity continued to increase with further doping and reached a value of 9×10^{-8} S cm^{-1} at 4.0 V vs Li^+/Li. On the other hand, P3HT/PEO showed a constant ionic conductivity of 4×10^{-7} S cm^{-1} across the examined potential window (Figure 2d). Thus, we may conclude that most of the ionic transport is supported by the flexible and ion-solvating ethylene oxide groups of PEO consistent with expectations from previous reports.[55] PEDOT:PSS showed an ionic conductivity of 4×10^{-5} to 6×10^{-5} S cm^{-1} in the

potential window of 3.2 to 4.0 V vs Li^+/Li. This value of ionic conductivity agrees closely with previous reports in the literature for PEDOT:PSS.[44] The ionic conductivity of un-doped P(NDI2OD-T2) at 2.4 V was 3×10^{-10} S cm^{-1} (Figure 4b).

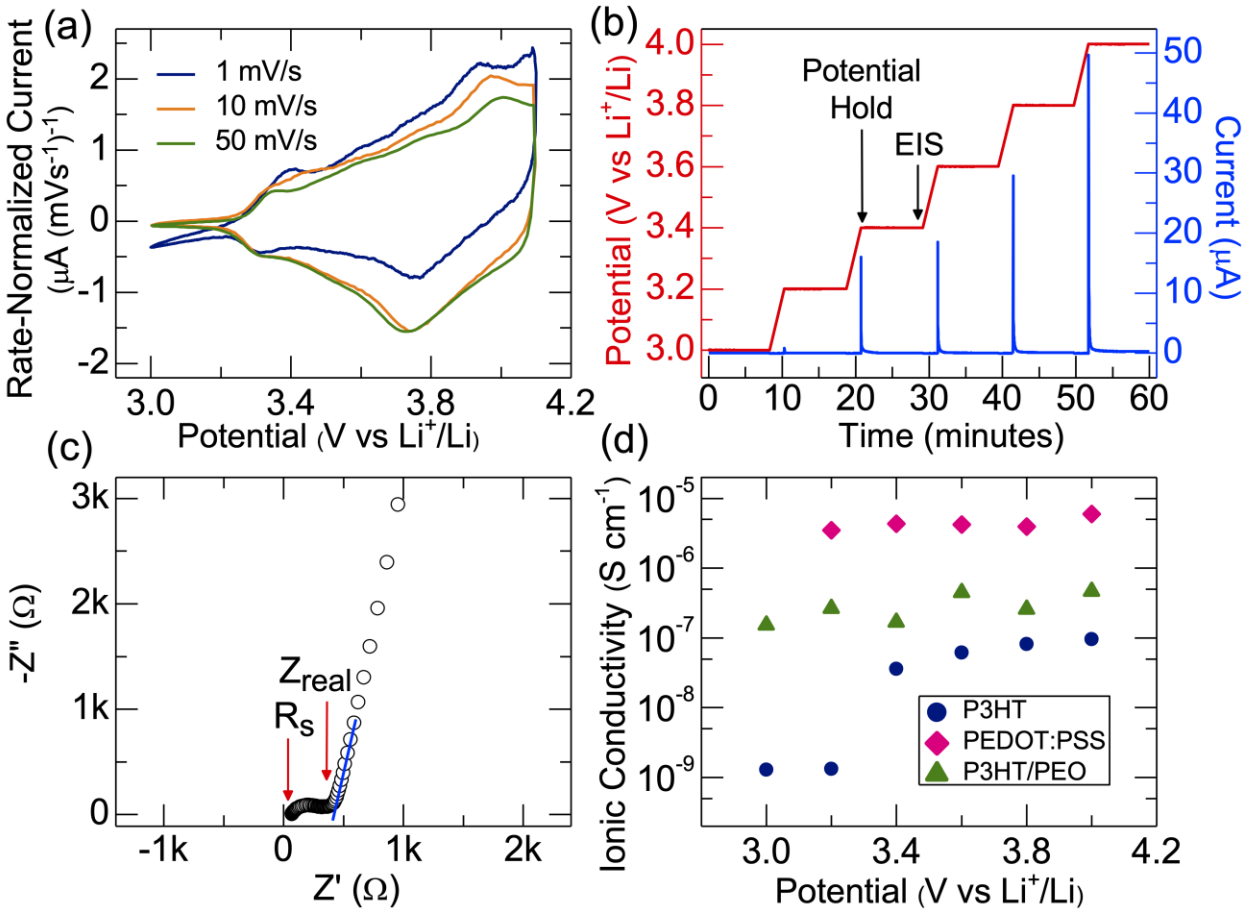

Figure 2. (a) Cyclic voltammetry plot of P3HT at various scan rates. (b) Electrochemical doping and impedance measurement protocol to determine ionic conductivity. (c) A representative Nyquist plot of P3HT obtained at 3.8V vs Li^+/Li using the three-electrode configuration. (d) Ionic conductivities of P3HT, PEDOT:PSS, and P3HT/PEO.

The ionic conductivity increased with electrochemical n-doping to reach 6×10^{-9} S cm^{-1} as the electrode was held at more negative potentials up to 1.6 V vs. Li^+/Li (Figure 4b). Thus, an increase

in ionic conductivity of at least two orders of magnitude was observed with both p-doped and n-doped polymers upon electrochemical doping. Thus, the effect of electrochemical doping was to increase the ionic conductivity.

Electronic Conductivity Measurements. The Nyquist plot in the two-electrode configuration (Figure 3c) showed two semicircular arcs. The impedance data was analyzed by the method of Huggins[56] for mixed conductors. Specifically, the data was fitted to the Debye equivalent circuit model for mixed conduction through the film (Figure 3b).[57] This equivalent circuit embodies the mixed electronic and ionic conductivity including the capacitance properties of the film. At high frequencies, the current flow occurs through the charge and discharge across the capacitive elements. At low frequencies, the electrodes block the ionic current, while the electronic current can still flow between the two terminals of the interdigitated gold electrodes. Such a circuit yields an impedance response with two semi-circles (Figure 3c). The diameter of the semicircle observed at the higher frequencies corresponded to a parallel combination of the ionic and electronic resistances, while the intersection of the second semicircle with the real axis at lower frequencies corresponded to the electronic resistance of the conducting polymer film, R_e. The electronic conductivity of the polymer film, σ_e, was then calculated based on the two-electrode geometry (Eq. 3**)** that is different from that applied to the ionic conductivity measurement.

$$\sigma_e = \frac{1}{R_e} \times \frac{d}{l \times (N-1) \times h} \tag{3}$$

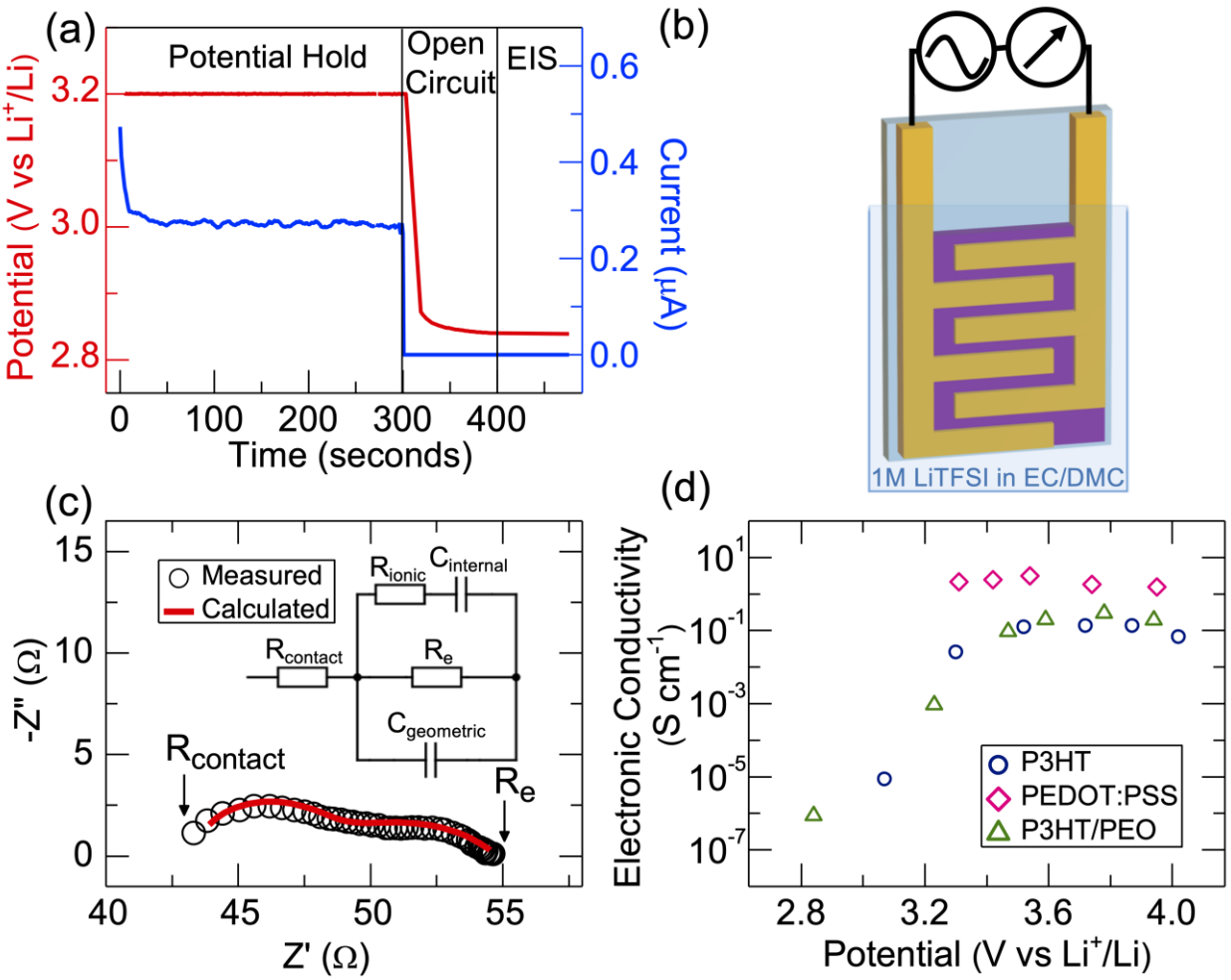

Figure 3. (a) Potential and current profiles during electrochemical doping preceding the EIS measurement protocol to determine electronic conductivity. (b) The two-electrode configuration used to measure the electronic conductivity of the polymer as a function of voltage. (c) A representative Nyquist impedance plot of P3HT obtained at 3.3 V vs Li^+/Li using the two-electrode configuration and the fitting circuit (inset) used to obtain the electronic conductivity. (d) Electronic conductivities of P3HT, PEDOT:PSS, and P3HT/PEO.

Effect of electrochemical doping. The electronic conductivity of P3HT in the un-doped state was determined to be 8×10^{-6} S cm^{-1} at 3.0 V vs Li^+/Li (Figure 3d). This value is in agreement with previously reported values from four-point probe measurements.[58] The electronic conductivity of P3HT however increased by several orders of magnitude upon electrochemical doping and reached a maximum of 1×10^{-1} S cm^{-1} at 3.5 V and remained constant until 3.9 V. The electronic conductivity then decreased slightly upon further electrochemical doping to 7×10^{-2} S cm^{-1} at 4.0 V vs Li^+/Li. The significant change in P3HT film impedance as a function of electrochemical doping is reflected in the Bode plots (Figure S10). The electronic conductivity of P3HT/PEO, as expected, was similar to that of P3HT when measured as a function of electrode potential. This trend showed that electron transport in P3HT was not negatively affected upon mixing with PEO. The electronic conductivity of PEDOT:PSS was determined to be 2 S cm^{-1}. This value is in agreement with the literature reports using a four-point probe method.[44] The electronic conductivity remained stable over the potential window investigated with only a slight decrease to 1 S cm^{-1} above 3.5 V vs Li^+/Li (Figure 3b). The electronic conductivity of un-doped P(NDI2OD-T2) was determined to be 5×10^{-7} S cm^{-1} (Figure 4b). This electronic conductivity increased to 5×10^{-4} S cm^{-1} as the polymer film was electrochemically doped by polarizing to 1.7 V vs Li^+/Li. Although the electronic conductivity of P(NDI2OD-T2) as a function of the degree of doping has not been previously reported, the observed value agrees with that for chemically-doped P(NDI2OD-T2) measured by four-point probe method.[46]

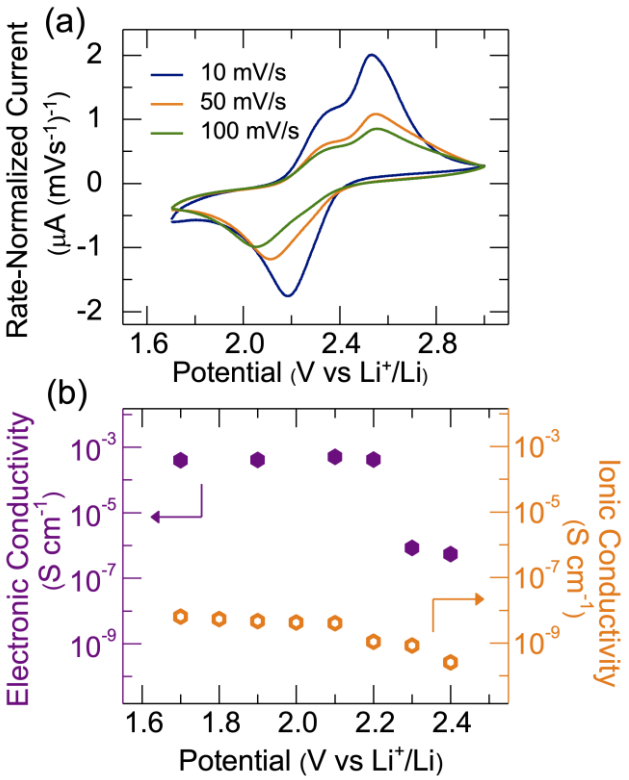

Figure 4. Cyclic voltammetry plot of P(NDI2OD-T2) at the various scan rates indicated. (b) The electronic and ionic conductivities of P(NDI2OD-T2) as a function of electrode potential.

CONCLUSIONS

In summary, we have demonstrated that the electronic and ionic conductivity of p-dopable and n-dopable conductive polymers can be reliably measured in LIB electrolyte solutions as a function of electrochemical doping by using EIS measurements on interdigitated electrodes in two geometric configurations. This technique is sensitive and robust despite the conductivity values changing by several orders of magnitude with doping. Although the determination of these charge-transport properties under electrochemical polarization is critical to the design of conductive polymers as additives and binders for electrodes in lithium-ion batteries, comprehensive measurements have been hitherto inaccessible. To validate the technique, the ionic and electronic conductivity for typical p-dopable polymers such as P3HT, P3HT/PEO, and PEDOT:PSS and a

model n-dopable polymer, P(NDI2OD-T2) was determined over the relevant potential windows in lithium-ion battery electrolyte. We have found that upon electrochemical doping, the electronic conductivity changes by more than five orders and the ionic conductivity by two orders of magnitude. As we are able to measure these charge transport properties in relevant electrolytes at various potentials, the method demonstrated here can become a useful tool for gaining insight into the in situ behavior of conductive polymers in various types of rechargeable batteries and other electrochemical devices.

ASSOCIATED CONTENT

Supporting Information. Polymer materials (SI-1), polymer structures (Figure S1), monomer and polymer synthesis (SI-2), physical characterization details (SI-3), NMR spectra (SI-4), electrode geometries and equivalent circuit for impedance measurements (SI-5), and electrochemical cycling and impedance data (SI-6)

AUTHOR INFORMATION

Corresponding Author

Sri R. Narayan. E-mail: sri.narayan@usc.edu

Author Contributions

The manuscript was written through contributions of all authors. All authors have given approval to the final version of the manuscript.

Notes

The authors declare no competing financial interest.

ACKNOWLEDGMENT

This work was supported as part of the Center for Synthetic Control Across Length-Scales for Advancing Rechargeables (SCALAR), an Energy Frontier Research Center funded by the U. S. Department of Energy, Office of Science, Basic Energy Sciences under Award #DE-SC0019381. Billal Zayat and Pratyusha Das acknowledge USC Dornsife Graduate Student Fellowships. The authors also acknowledge the Loker Hydrocarbon Research Institute and USC's Core Center of Excellence in Nano Imaging.

REFERENCES

(1) Yang, Z.; Zhang, J.; Kintner-Meyer, M. C.; Lu, X.; Choi, D.; Lemmon, J. P.; Liu, J. Electrochemical Energy Storage for Green Grid. *Chem. Rev.* **2011,** 111, 3577-3613.

(2) Thackeray, M. M.; Wolverton, C.; Isaacs, E. D. Electrical Energy Storage for Transportation—Approaching the Limits of, and Going Beyond, Lithium-Ion Batteries. *Energy Environ. Sci.* **2012,** 5, 7854-7863.

(3) Dunn, B.; Kamath, H.; Tarascon, J. M. Electrical Energy Storage for the Grid: A Battery of Choices. *Science* **2011,** 334, 928-935.

(4) Chen, H.; Ling, M.; Hencz, L.; Ling, H. Y.; Li, G.; Lin, Z.; Liu, G.; Zhang, S. Exploring Chemical, Mechanical, and Electrical Functionalities of Binders for Advanced Energy-Storage Devices. *Chem. Rev.* **2018,** 118, 8936-8982.

(5) Dudney, N. J.; Li, J. Using All Energy in a Battery. *Science* **2015,** 347, 131-132.

(6) Lopez, J.; Mackanic, D. G.; Cui, Y.; Bao, Z. Designing Polymers for Advanced Battery Chemistries. *Nat. Rev. Mater.* **2019,** 4, 312-330.

(7) Patnaik, S. G.; Vedarajan, R.; Matsumi, N. BIAN Based Functional Diimine Polymer Binder for High Performance Li Ion Batteries. *J. Mater. Chem. A* **2017,** 5, 17909-17919.

(8) Park, S.-J.; Zhao, H.; Ai, G.; Wang, C.; Song, X.; Yuca, N.; Battaglia, V. S.; Yang, W.; Liu, G. Side-Chain Conducting and Phase-Separated Polymeric Binders for High-Performance Silicon Anodes in Lithium-Ion Batteries. *J. Am. Chem. Soc.* **2015,** 137, 2565-2571.

(9) Cao, Y.; Qi, X.; Hu, K.; Wang, Y.; Gan, Z.; Li, Y.; Hu, G.; Peng, Z.; Du, K. Conductive Polymers Encapsulation to Enhance Electrochemical Performance of Ni-Rich Cathode Materials for Li-Ion Batteries. *ACS Appl. Mater. Interfaces* **2018,** 10, 18270-18280.

(10) Kwon, Y. H.; Minnici, K.; Lee, S. R.; Zhang, G.; Takeuchi, E. S.; Takeuchi, K. J.; Marschilok, A. C.; Reichmanis, E. SWNT Networks with Polythiophene Carboxylate Links for High-Performance Silicon Monoxide Electrodes. *ACS Appl. Energy Mater.* **2018,** 1, 2417-2423.

(11) Wu, M.; Xiao, X.; Vukmirovic, N.; Xun, S.; Das, P. K.; Song, X.; Olalde-Velasco, P.; Wang, D.; Weber, A. Z.; Wang, L.-W. Toward an Ideal Polymer Binder Design for High-Capacity Battery Anodes. *J. Am. Chem. Soc.* **2013,** 135, 12048-12056.

(12) Salem, N.; Lavrisa, M.; Abu-Lebdeh, Y. Ionically-Functionalized Poly(thiophene) Conductive Polymers as Binders for Silicon and Graphite Anodes for Li-Ion Batteries. *Energy Technol.* **2016,** 4, 331-340.

(13) Wu, H.; Yu, G.; Pan, L.; Liu, N.; McDowell, M. T.; Bao, Z.; Cui, Y. Stable Li-Ion Battery Anodes by in-Situ Polymerization of Conducting Hydrogel to Conformally Coat Silicon Nanoparticles. *Nat. Commun.* **2013,** 4, 1-6.

(14) Zhao, H.; Wang, Z.; Lu, P.; Jiang, M.; Shi, F.; Song, X.; Zheng, Z.; Zhou, X.; Fu, Y.; Abdelbast, G. Toward Practical Application of Functional Conductive Polymer Binder for a High-Energy Lithium-Ion Battery Design. *Nano Lett.* **2014,** 14, 6704-6710.

(15) Higgins, T. M.; Park, S.-H.; King, P. J.; Zhang, C.; McEvoy, N.; Berner, N. C.; Daly, D.; Shmeliov, A.; Khan, U.; Duesberg, G.; Nicolosi, V.; Coleman, J. N. A Commercial Conducting Polymer as Both Binder and Conductive Additive for Silicon Nanoparticle-Based Lithium-Ion Battery Negative Electrodes. *ACS Nano* **2016,** 10, 3702-3713.

(16) Kim, J.-M.; Park, H.-S.; Park, J.-H.; Kim, T.-H.; Song, H.-K.; Lee, S.-Y. Conducting Polymer-Skinned Electroactive Materials of Lithium-Ion Batteries: Ready for Monocomponent Electrodes without Additional Binders and Conductive Agents. *ACS Appl. Mater. Interfaces* **2014,** 6, 12789-12797.

(17) Kwon, Y. H.; Minnici, K.; Park, J. J.; Lee, S. R.; Zhang, G.; Takeuchi, E. S.; Takeuchi, K. J.; Marschilok, A. C.; Reichmanis, E. SWNT Anchored with Carboxylated Polythiophene "Links" on High-Capacity Li-Ion Battery Anode Materials. *J. Am. Chem. Soc.* **2018,** 140, 5666-5669.

(18) Ling, M.; Qiu, J.; Li, S.; Yan, C.; Kiefel, M. J.; Liu, G.; Zhang, S. Multifunctional SA-PProDOT Binder for Lithium Ion Batteries. *Nano Lett.* **2015,** 15, 4440-4447.

(19) Yao, Y.; Liu, N.; McDowell, M. T.; Pasta, M.; Cui, Y. Improving the Cycling Stability of Silicon Nanowire Anodes with Conducting Polymer Coatings. *Energy Environ. Sci.* **2012,** 5, 7927-7930.

(20) Zeng, W.; Wang, L.; Peng, X.; Liu, T.; Jiang, Y.; Qin, F.; Hu, L.; Chu, P. K.; Huo, K.; Zhou, Y. Enhanced Ion Conductivity in Conducting Polymer Binder for High-Performance Silicon Anodes in Advanced Lithium-Ion Batteries. *Adv. Energy Mater.* **2018,** 8, 1702314.

(21) Zhao, H.; Fu, Y.; Ling, M.; Jia, Z.; Song, X.; Chen, Z.; Lu, J.; Amine, K.; Liu, G. Conductive Polymer Binder-Enabled SiO–$Sn_xCo_yC_z$ Anode for High-Energy Lithium-Ion Batteries. *ACS Appl. Mater. Interfaces* **2016,** 8, 13373-13377.

(22) Zhao, H.; Wang, Z.; Lu, P.; Jiang, M.; Shi, F.; Song, X.; Zheng, Z.; Zhou, X.; Fu, Y.; Abdelbast, G.; Xiao, X.; Liu, Z.; Battaglia, V. S.; Zaghib, K.; Liu, G. Toward Practical Application of Functional Conductive Polymer Binder for a High-Energy Lithium-Ion Battery Design. *Nano Lett.* **2014,** 14, 6704-6710.

(23) Zhong, H.; He, A.; Lu, J.; Sun, M.; He, J.; Zhang, L. Carboxymethyl Chitosan/Conducting Polymer as Water-Soluble Composite Binder for $LiFePO_4$ Cathode in Lithium Ion Batteries. *J. Power Sources* **2016,** 336, 107-114.

(24) Kim, S.-M.; Kim, M. H.; Choi, S. Y.; Lee, J. G.; Jang, J.; Lee, J. B.; Ryu, J. H.; Hwang, S. S.; Park, J.-H.; Shin, K. Poly (Phenanthrenequinone) as a Conductive Binder for Nano-Sized Silicon Negative Electrodes. *Energy Environ. Sci.* **2015,** 8, 1538-1543.

(25) Chen, H.; Dong, W.; Ge, J.; Wang, C.; Wu, X.; Lu, W.; Chen, L. Ultrafine Sulfur Nanoparticles in Conducting Polymer Shell as Cathode Materials for High Performance Lithium/Sulfur Batteries. *Sci. Rep.* **2013,** 3, 1910.

(26) Fong, K. D.; Wang, T.; Kim, H.-K.; Kumar, R. V.; Smoukov, S. K. Semi-Interpenetrating Polymer Networks for Enhanced Supercapacitor Electrodes. *ACS Energy Lett.* **2017,** 2, 2014-2020.

(27) Knoche, K. L.; Hickey, D. P.; Milton, R. D.; Curchoe, C. L.; Minteer, S. D. Hybrid Glucose/O_2 Biobattery and Supercapacitor Utilizing a Pseudocapacitive Dimethylferrocene Redox Polymer at the Bioanode. *ACS Energy Lett.* **2016,** 1, 380-385.

(28) Tsao, Y.; Chen, Z.; Rondeau-Gagne, S.; Zhang, Q.; Yao, H.; Chen, S.; Zhou, G.; Zu, C.; Cui, Y.; Bao, Z. Enhanced Cycling Stability of Sulfur Electrodes through Effective Binding of Pyridine-Functionalized Polymer. *ACS Energy Lett.* **2017,** 2, 2454-2462.

(29) Bryan, A. M.; Santino, L. M.; Lu, Y.; Acharya, S.; D'Arcy, J. M. Conducting Polymers for Pseudocapacitive Energy Storage. *Chem. Mater.* **2016,** 28, 5989-5998.

(30) Xie, J.; Gu, P.; Zhang, Q. Nanostructured Conjugated Polymers: Toward High-Performance Organic Electrodes for Rechargeable Batteries. *ACS Energy Lett.* **2017,** 2, 1985-1996.

(31) Bertho, D.; Jouanin, C. Polaron and Bipolaron Excitations in Doped Polythiophene. *Phys. Rev. B* **1987,** 35, 626-633.

(32) Cao, J.; Curtis, M. D. Polarons, Bipolarons, and Π-Dimers of Bis (3, 4-Ethylene-Dioxythiophene)-(4, 4 '-Dialkyl-2, 2 '-Bithiazole)-co-Oligomers. Direct Measure of the Intermolecular Exciton Transfer Interaction. *Chem. Mater.* **2003,** 15, 4424-4430.

(33) Patel, S. N.; Javier, A. E.; Balsara, N. P. Electrochemically Oxidized Electronic and Ionic Conducting Nanostructured Block Copolymers for Lithium Battery Electrodes. *ACS Nano* **2013,** 7, 6056-6068.

(34) Lai, C. H.; Ashby, D. S.; Lin, T. C.; Lau, J.; Dawson, A.; Tolbert, S. H.; Dunn, B. S. Application of Poly(3-Hexylthiophene-2,5-Diyl) as a Protective Coating for High Rate Cathode Materials. *Chem. Mater.* **2018,** 30, 2589-2599.

(35) Manley, E. F.; Strzalka, J.; Fauvell, T. J.; Jackson, N. E.; Leonardi, M. J.; Eastham, N. D.; Marks, T. J.; Chen, L. X. In Situ Giwaxs Analysis of Solvent and Additive Effects on PTB7 Thin Film Microstructure Evolution During Spin Coating. *Adv. Mater.* **2017,** 29, 1703933.

(36) Fontana, M. T.; Kang, H.; Yee, P. Y.; Fan, Z.; Hawks, S. A.; Schelhas, L. T.; Subramaniyan, S.; Hwang, Y.-J.; Jenekhe, S. A.; Tolbert, S. H. Low-Vapor-Pressure Solvent Additives Function as Polymer Swelling Agents in Bulk Heterojunction Organic Photovoltaics. *J. Phys. Chem. C* **2018,** 122, 16574-16588.

(37) Liu, J.; Shi, Y.; Dong, J.; Nugraha, M. I.; Qiu, X.; Su, M.; Chiechi, R. C.; Baran, D.; Portale, G.; Guo, X.; Koster, L. J. A. Overcoming Coulomb Interaction Improves Free-Charge Generation and Thermoelectric Properties for N-Doped Conjugated Polymers. *ACS Energy Lett.* **2019,** 4, 1556-1564.

(38) Liu, J.; Qiu, L.; Portale, G.; Koopmans, M.; Ten Brink, G.; Hummelen, J. C.; Koster, L. J. A. N-Type Organic Thermoelectrics: Improved Power Factor by Tailoring Host-Dopant Miscibility. *Adv. Mater.* **2017,** 29, 1701641.

(39) Choi, J.; Kim, K.-H.; Yu, H.; Lee, C.; Kang, H.; Song, I.; Kim, Y.; Oh, J. H.; Kim, B. J. Importance of Electron Transport Ability in Naphthalene Diimide-Based Polymer Acceptors for High-Performance, Additive-Free, All-Polymer Solar Cells. *Chem. Mater.* **2015,** 27, 5230-5237.

(40) DuBois, C.; Reynolds, J. R. 3, 4-Ethylenedioxythiophene–Pyridine-Based Polymers: Redox or N-Type Electronic Conductivity? *Adv. Mater.* **2002,** 14, 1844-1846.

(41) Farhat, T. R.; Hammond, P. T. Engineering Ionic and Electronic Conductivity in Polymer Catalytic Electrodes Using the Layer-by-Layer Technique. *Chem. Mater.* **2006,** 18, 41-49.

(42) Morales, J.; Olayo, M.; Cruz, G.; Castillo-Ortega, M.; Olayo, R. Electronic Conductivity of Pyrrole and Aniline Thin Films Polymerized by Plasma. *J. Polym. Sci., Part B: Polym. Phys.* **2000,** 38, 3247-3255.

(43) Ochmanska, J.; Pickup, P. G. Conducting Polypyrrole Films Containing [Ru (2, 2'-Bipyridine)$_2$(3-{Pyrrol-1-Ylmethyl} Pyridine) Cl]$^+$: Electrochemistry, Spectroelectrochemistry, Electronic Conductivity, and Ionic Conductivity. *J. Electroanal. Chem. Interf. Electrochem.* **1989,** 271, 83-105.

(44) McDonald, M. B.; Hammond, P. T. Efficient Transport Networks in a Dual Electron/Lithium-Conducting Polymeric Composite for Electrochemical Applications. *ACS Appl. Mater. Interfaces* **2018,** 10, 15681-15690.

(45) Dong, B. X.; Nowak, C.; Onorato, J. W.; Strzalka, J.; Escobedo, F. A.; Luscombe, C. K.; Nealey, P. F.; Patel, S. N. Influence of Side-Chain Chemistry on Structure and Ionic Conduction Characteristics of Polythiophene Derivatives: A Computational and Experimental Study. *Chem. Mater.* **2019,** 31, 1418-1429.

(46) Liu, J.; Qiu, L.; Alessandri, R.; Qiu, X.; Portale, G.; Dong, J. J.; Talsma, W.; Ye, G.; Sengrian, A. A.; Souza, P. C. T.; Loi, M. A.; Chiechi, R. C.; Marrink, S. J.; Hummelen, J. C.; Koster, L. J. A. Enhancing Molecular N-Type Doping of Donor–Acceptor Copolymers by Tailoring Side Chains. *Adv. Mater.* **2018,** 30, 1704630.

(47) Patel, S. N.; Javier, A. E.; Stone, G. M.; Mullin, S. A.; Balsara, N. P. Simultaneous Conduction of Electronic Charge and Lithium Ions in Block Copolymers. *ACS Nano* **2012,** 6, 1589-1600.

(48) Enengl, C.; Enengl, S.; Pluczyk, S.; Havlicek, M.; Lapkowski, M.; Neugebauer, H.; Ehrenfreund, E. Doping-Induced Absorption Bands in P3HT: Polarons and Bipolarons. *Chemphyschem* **2016,** 17, 3836-3844.

(49) Bisquert, J.; Belmonte, G. G.; Santiago, F. F.; Ferriols, N. S.; Yamashita, M.; Pereira, E. C. Application of a Distributed Impedance Model in the Analysis of Conducting Polymer Films. *Electrochem. Commun.* **2000,** 2, 601-605.

(50) Bisquert, J.; Garcia-Belmonte, G.; Fabregat-Santiago, F.; Ferriols, N. S.; Bogdanoff, P.; Pereira, E. C. Doubling Exponent Models for the Analysis of Porous Film Electrodes by Impedance. Relaxation of TiO_2 Nanoporous in Aqueous Solution. *J. Phys. Chem. B* **2000,** 104, 2287-2298.

(51) Garcia-Belmonte, G.; Bisquert, J.; Pereira, E. C.; Fabregat-Santiago, F. Switching Behaviour in Lightly Doped Polymeric Porous Film Electrodes. Improving Distributed Impedance Models for Mixed Conduction Conditions. *J. Electroanal. Chem.* **2001,** 508, 48-58.

(52) Albery, W. J.; Chen, Z.; Horrocks, B. R.; Mount, A. R.; Wilson, P. J.; Bloor, D.; Monkman, A. T.; Elliott, C. M. Spectroscopic and Electrochemical Studies of Charge Transfer in Modified Electrodes. *Faraday Discuss.* **1989,** 88, 247-259.

(53) Rubinstein, I.; Rishpon, J.; Gottesfeld, S. An Ac-Impedance Study of Electrochemical Processes at Nafion-Coated Electrodes. *J. Electrochem. Soc.* **1986,** 133, 729-734.

(54) Pickup, P. G. Alternating Current Impedance Study of a Polypyrrole-Based Anion-Exchange Polymer. *J. Chem. Soc., Faraday Trans.* **1990,** 86, 3631-3636.

(55) Fergus, J. W., Ceramic and Polymeric Solid Electrolytes for Lithium-Ion Batteries. In 2010; Vol. 195, pp 4554-4569.

(56) Huggins, R. A. Simple Method to Determine Electronic and Ionic Components of the Conductivity in Mixed Conductors a Review. *Ionics* **2002,** 8, 300-313.

(57) Jamnik, J. Treatment of the Impedance of Mixed Conductors Equivalent Circuit Model and Explicit Approximate Solutions. *J. Electrochem. Soc.* **1999,** 146, 4183-4183.

(58) Obrzut, J.; Page, K. A. Electrical Conductivity and Relaxation in Poly(3-Hexylthiophene). *Phys. Rev. B* **2009,** 80, 195211.

SYNOPSIS

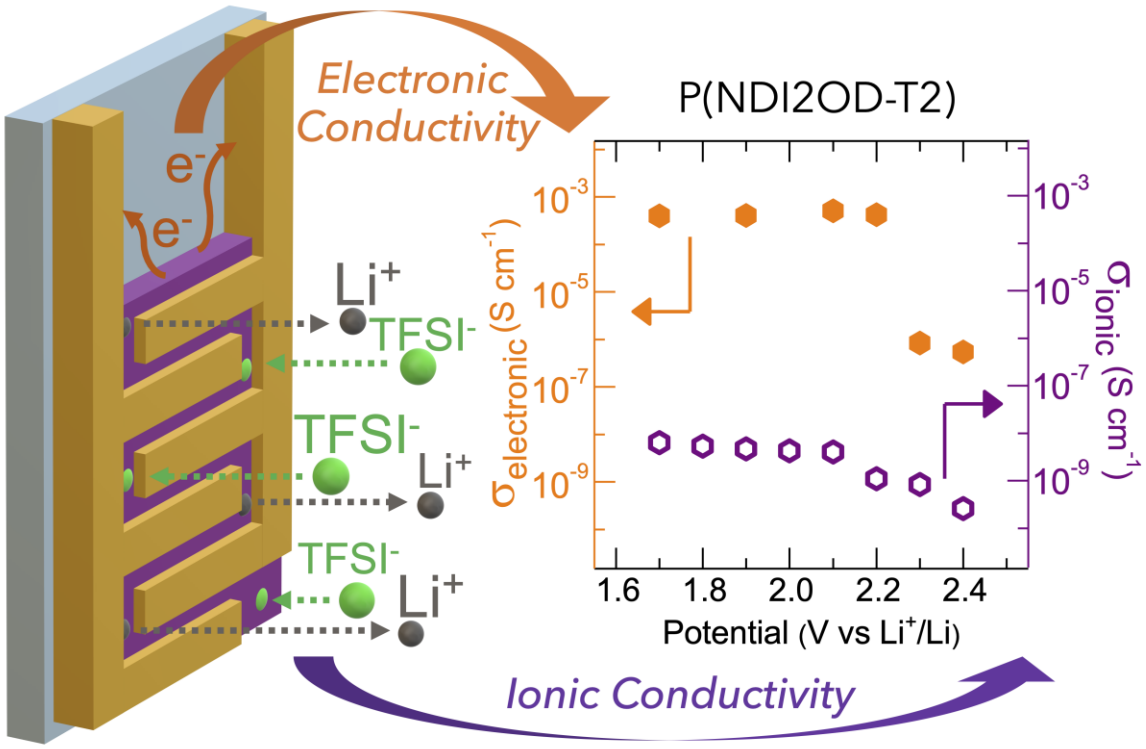
Electronic Conductivity
e-
e-
Li+
TFSI-
TFSI-
Li+
TFSI-
Li+
P(NDI2OD-T2)
σelectronic (S cm-1)
σionic (S cm-1)
10-3
10-5
10-7
10-9
1.6
1.8
2.0
2.2
2.4
Potential (V vs Li+/Li)
Ionic Conductivity